

# GPS-derived Velocity and Crustal Strain Field in the Suez-Sinai Area, Egypt

Gamal El-Fiky\*

Construction Eng. & Utilities Department, Faculty of Eng., Zagazig University, Zagazig, Egypt

## Abstract

Five GPS measurements collected in campaign mode during the period 1997~2002 are analyzed to derive velocity vectors and principal components of crustal strains along the Gulf of Suez and in the southern part of the Sinai Peninsula, Egypt. Estimated horizontal velocity vectors in ITRF2000 are found to be in the range of 29~35 mm/yr with an uncertainty level in the order of 1~2 mm/yr (95% confidence level). Then, estimated velocities are converted into a kinematic reference frame (Prawirodirdjo and Bock, 2004) to discuss crustal deformation relative to the Eurasian plate. Least-Squares prediction (LSP) technique is employed to segregate signal and noise from velocity vectors. Estimated signals are used to reconstruct strains, dilatations, maximum shear strains, and principal axes of strains. Strains obtained might portray active tectonic environments in the region under study. (1) Dilatational strains indicate that the region under study is mainly divided into two areas : the western part around the Gulf of Suez where extensional strain is predominant, and the eastern part around the Gulf of Aqaba where compressional strains prevail. (2) Maximum shear strain is mostly accommodated at the Gulf of Suez and Gulf of Aqaba. Distribution of seismicity shows high consistency with high shear strain areas. The estimated dilatation strain rate and the maximum shear strain rate are both 0.25 Micro-strain/yr on average. (3) Principal axes of the strains indicate that an extensional force is acting along the Gulf of Suez in the NE-SW direction. Moreover, the principal axes of strains show a good correlation with the  $S_{Hmax}$  directions obtained from earthquake focal mechanisms and borehole breakouts.

**Key words :** Sinai Peninsula, Gulf of Suez, Gulf of Aqaba, GPS measurements, crustal strains, least-squares prediction.

## 1. Introduction

The territory of Egypt is not a major seismic zone (e.g., Ambraseys *et al.*, 1994), but earthquakes represent a significant hazard. Egypt covers an area of about 1,000,000 km<sup>2</sup>, and is located at the northeastern corner of the African plate (Fig. 1). The African plate is bounded at the east by the Arabian plate and at the north by the Eurasian/Anatolian plate (Fig. 2). The boundaries between these plates are in relative movement with respect to each other. The Arabian plate is moving in the NNW direction relative to the Eurasian plate at a rate of about 20~25 mm/yr (DeMets *et al.*, 1990 ; DeMets *et al.*, 1994 ; Jestin *et al.*, 1994), causing crustal spreading along the axis of the Red Sea and lateral slip along the Dead Sea trans-

form zone, producing the Gulf of Aqaba - Dead Sea-East Anatolian trend. The African plate is moving in the northward direction relative to the Eurasian plate at a rate of about 10 mm/yr (DeMets *et al.*, 1990 ; DeMets *et al.*, 1994). The differential motion between Africa and Arabia (10~15 mm/yr) is thought to be taken up predominantly by a left-lateral motion along the Dead Sea transform fault (McClusky *et al.*, 2000, El-Fiky, 2000).

The African continent is considered to be a stable region, with the exception of the East African Rift, which branches in northern Ethiopia into the Red Sea Rift and the Gulf of Aden Rift (e.g., Garfunkel, 1981). The Red Sea Rift branches into the Gulf of Suez and the Gulf of Aqaba. The Sinai Peninsula is

\* e-mail: gamal\_elfiky@yahoo.com

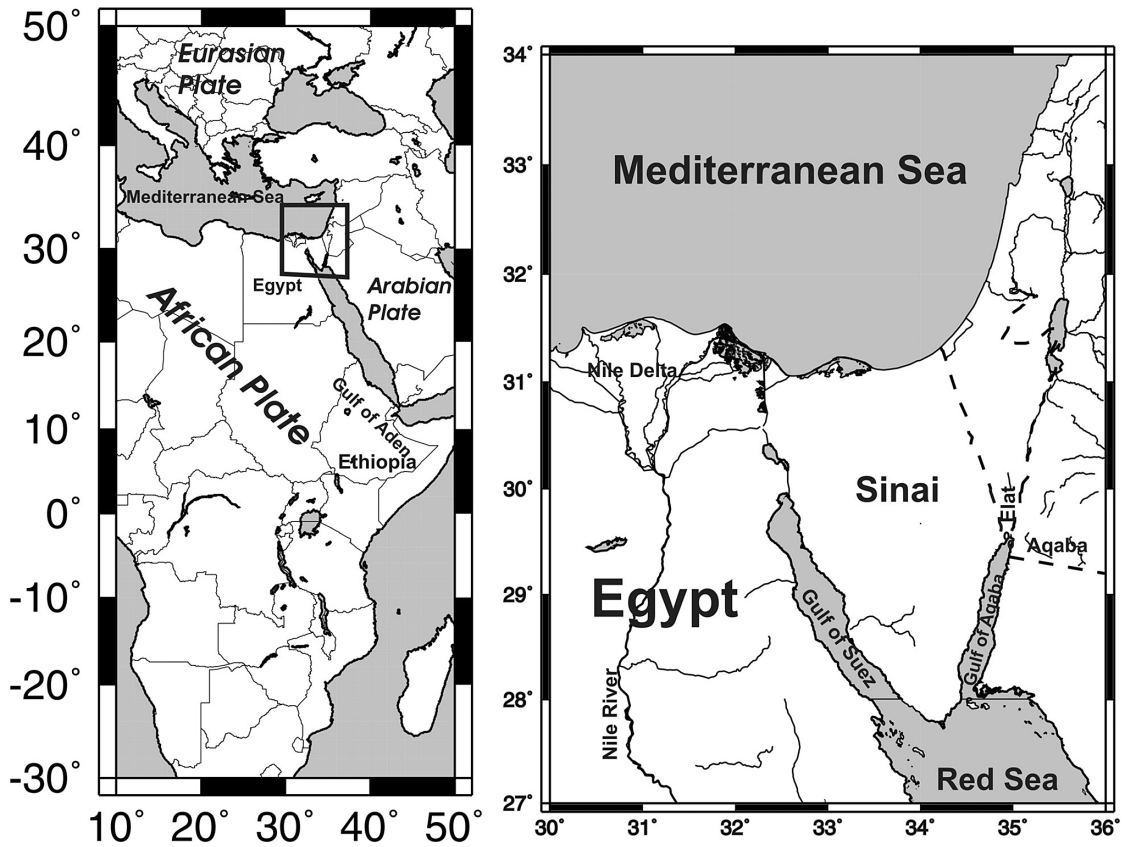


Fig. 1. Location map of Egypt and area of study.

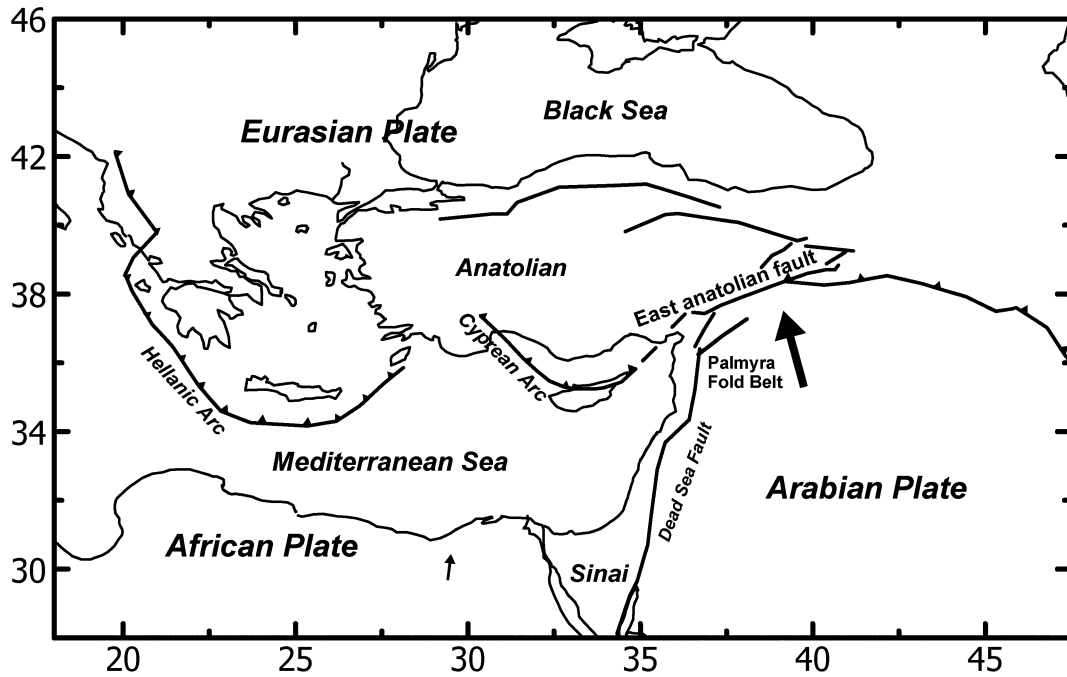


Fig. 2. Simplified tectonic map of the Eastern Mediterranean and the Middle East region. Arrows indicate relative plate motion by NUVEL-1A (DeMets et al., 1994).

one of the main geographic units of Egypt. It is located north of the Red Sea, and is wedged between the Aqaba and Suez Gulfs in the northeastern part of Egypt, southeast of the Mediterranean Sea (Fig. 1). Most historical and recent seismic activities in the Sinai area were recorded at the northern part of the Red Sea, southern part of Gulf of Suez, and the Gulf of Aqaba (Kebeasy, 1990) (Fig. 3).

GPS finds applications in the crustal deformation studies because it gives very precise measure-

ments of a location. Depending upon the signal used from the GPS satellites, the software used, and the strategy applied, the resulting uncertainty of site location can be as large as several tens of meters, or as small as a few millimeters or less. The maximum precision is obtained when satellite signals from two receivers are combined. Phase information in the signal can be used to determine the position difference between sites with an accuracy of a few millimeters. GPS is also a technique that has sufficient

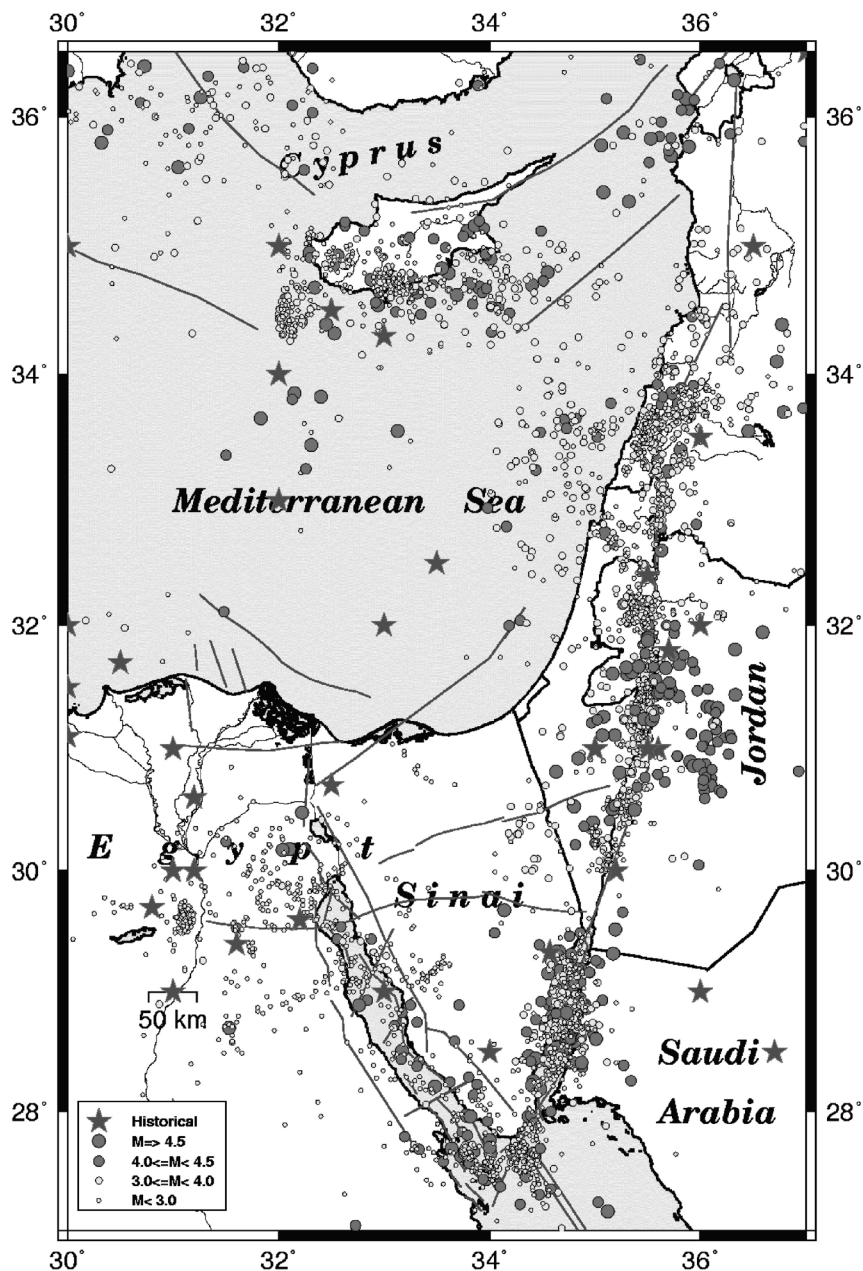


Fig. 3. A seismicity map of the Suez-Sinai region and surrounding areas (2200BC-1995) compiled from data of Badawy and Horvath, (1999).

accuracy to measure small motions produced by earthquake activity.

The aim of this paper is to shed light on the tectonics and the kinematics of the Sinai area by investigating crustal deformations of the region using GPS measurements for the period 1997~2002 with a network composed of 11 sites located on the west shore of the Gulf of Suez and the Sinai Peninsula.

## 2. Tectonic sketch of Sinai

The tectonics of the Sinai Peninsula are strongly dominated by the active boundaries between the African and the Arabian plates, which separate one from the other. According to current literature, from Neogene to Late Miocene, this area was subjected to different phases of motion. Initially, the northeastward drift of the Arabian Peninsula yielded the opening of the Red Sea; subsequently, the opening propagated toward the north along the Gulf of Suez area. Finally, the Gulf of Suez opening probably slowed and the stresses of the Red Sea rift were transferred along the Aqaba-Levant area, generating a NNE left shear with a minor extensional component (Fig. 2). Several geological and seismological investigations assert that the area surrounding the Gulf of Suez displayed, in the past, extensional tectonics with a large deformation rate (e.g., Steckler *et al.*, 1988; Le Pichon and Gaulier, 1988; Salamon *et al.*, 2003). At present, some extension is still recognized, but with a low deformation rate (Steckler, 1985; Steckler *et al.*, 1988).

The Sinai Peninsula has been recognized as a sub-plate of the African plate (Ben-Menahem *et al.*, 1976, Courtillot *et al.*, 1987) located at the triple junction of the Gulf of Suez rift, the Aqaba-Levant transform fault, and the Red Sea rift. The question of whether the triggered motion of the Aqaba-Levant fault has entirely or partially replaced the opening of Gulf of Suez is still under discussion. Recent studies show that the oldest movements of the Aqaba-Dead Sea fault are certainly younger than those in the Suez basin (Steckler *et al.*, 1988). According to these studies, the Gulf of Suez shows, at present, low rates of extensional features ( $< 2$  mm/yr) and tectonic subsidence (Steckler *et al.*, 1988); on the contrary, the Aqaba-Levant transform system displays a higher rate of motion with geological evidence suggesting

an average of about 8~9 mm/yr (Le Pichon and Gaulier, 1988). The Dead Sea fault system extends over about 450 km from the Gulf of Aqaba to the northern margin of the Hula Valley, where there is a complicated transition zone from the sinistral strike slip toward the thrust components of the Taurus arc.

Seismic activity mainly occurs along the borders of the Sinai sub-plate: in the southern part of the Gulf of Suez, along the Aqaba-Levant fault system, where it reaches the highest level, and along the Dead-Sea-Jordan transform. On the contrary, intra-plate seismicity is diffused and low (Fig. 4). Focal mechanisms characterize the Gulf of Suez solution with extensional features, and the Aqaba-Levant fault system with both left lateral strike slip and extensional styles (Fig. 4). Seismic activity in the Gulf of Suez is highest near its entrance. For example, a  $M_s$  6.6 earthquake occurred near Shadwan Island on March 31, 1969 and caused some damage, which included numerous rock falls (Ambrasey *et al.*, 1994). In the Gulf of Aqaba region, numerous moderate earthquakes with associated aftershock sequences and some earthquake swarms were experienced. An intensive earthquake swarm occurred during the period August 1993~February 1994, and was associated with more than 1,200 events (Kimata *et al.*, 1997). The largest earthquake occurred in the Gulf of Aqaba on November 22, 1995, with a magnitude of 7.0. Ground fractures, damage, collapsed buildings, and liquefaction were observed in Aqaba (Jordan), Elat (Israel), and along the western coast of the Gulf of Aqaba on the Sinai Peninsula (Fig. 1).

## 3. Data acquisition and analysis

GPS has found applications in crustal deformation studies since the early 1980s in various regions of the world. In the southern part of the Sinai Peninsula, GPS measurements were initiated in 1997. A GPS network consisting of 11 sites—seven located on the Sinai Peninsula and the other four on the west shore of the Gulf of Suez—has been established to investigate crustal deformations in this tectonically active region. Campaign observations have been repeated five times during the period from 1997 to 2002. The first campaign was carried out in 1997 from November 20 to December 2; the second was performed in 1998 from May 25 to 31; the third one was performed in 1999 from August 4 to 5; the fourth

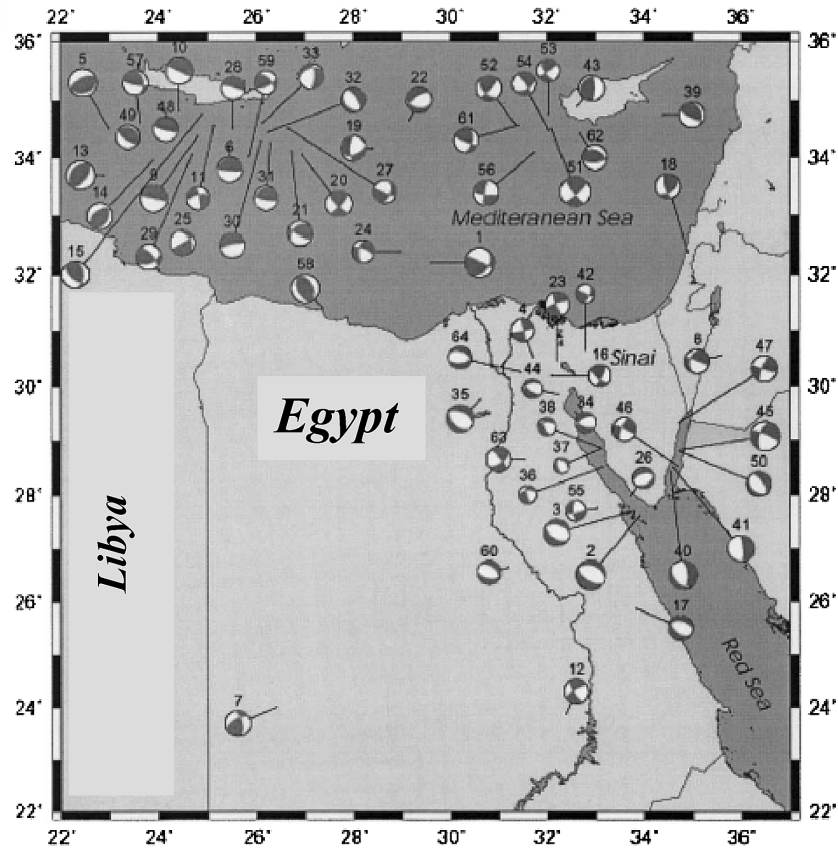


Fig. 4. Focal mechanisms of moderate to large earthquakes in the region under study and surrounding area for the period 1955~1999 (modified from Mahmoud, 2003).

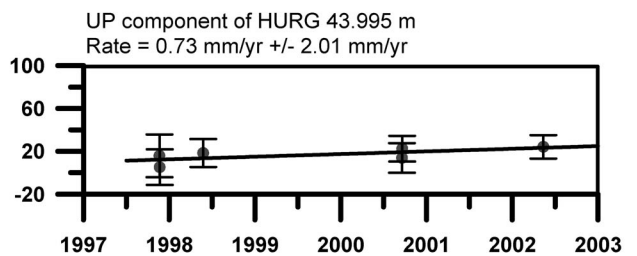
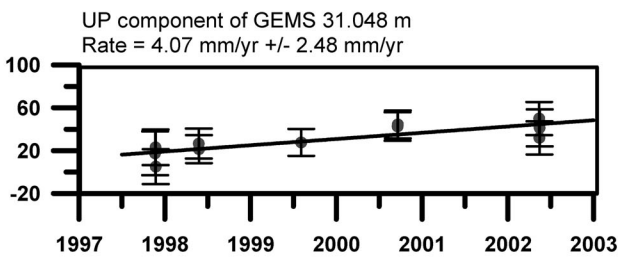
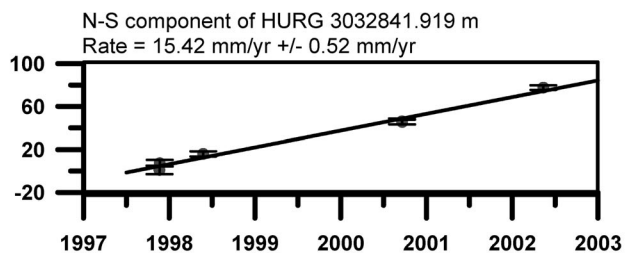
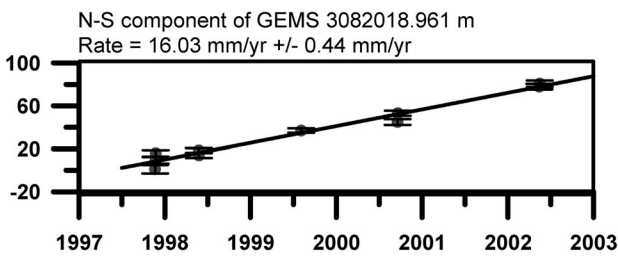
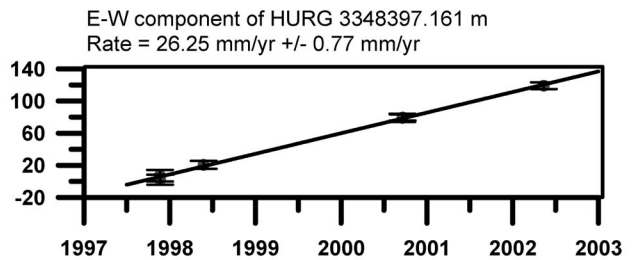
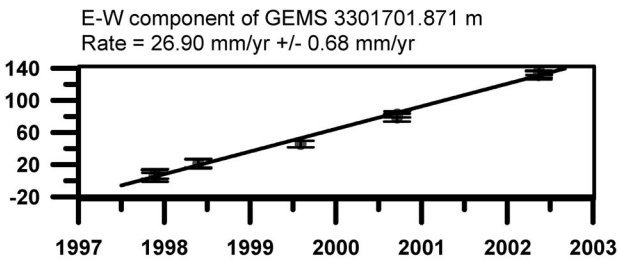
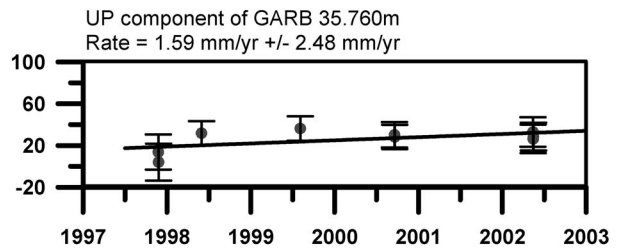
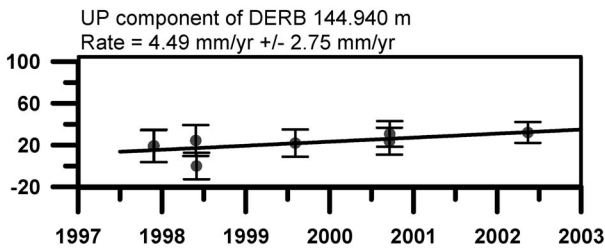
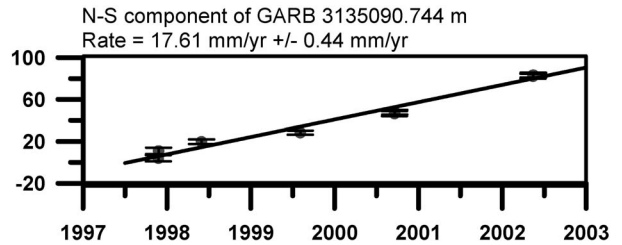
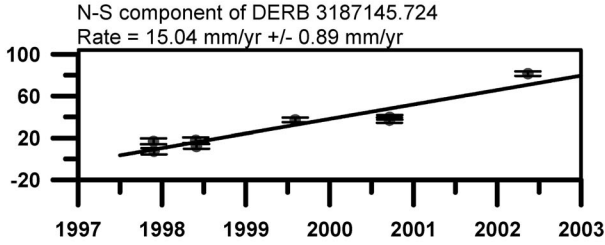
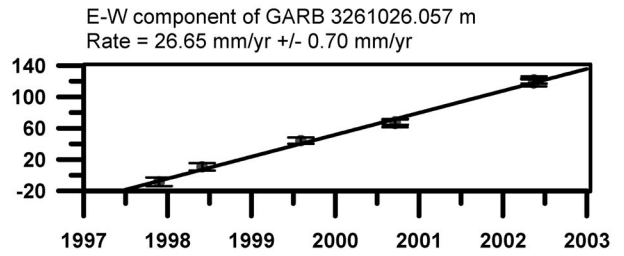
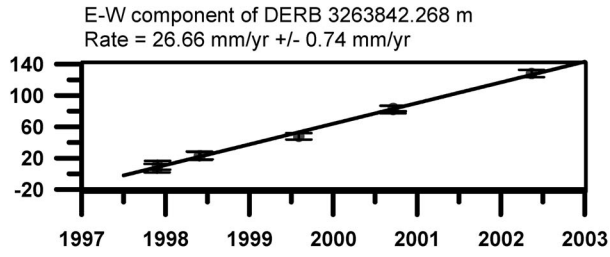
campaign was performed in 2000 from September 18 to 19 ; and the fifth one was performed in 2002 from 14 to 16 May. The data length spanning over six years might be long enough to obtain reliable velocities at sites (e.g., Kato *et al.*, 1998). GPS observations were carried out using dual frequency Trimble 4000 SSE and 4000SSI receivers. The sampling interval and the elevation were fixed at 30 sec and  $15^\circ$  respectively throughout the survey.

I processed pseudo-range and phase GPS data in single-day solutions using GAMIT/GLOBK software packages (King and Bock, 1997). For regional station coordinates, I solved satellite state vectors and phase ambiguities using doubly-differenced ionosphere-free LC GPS phase measurements. I used IGS final orbits and IERS Earth orientation parameters, and applied azimuth and elevation-dependent antenna phase center models, following the tables recommended by the IGS. In processing, I included seven stations of the International GPS service for Geodynamic (BAHR, ANKR, MADR, MAS1, MALI, RAMO,

HARK) to serve as ties with the International Terrestrial Reference Frame 2000 (ITRF2000, Altamimi *et al.*, 2002). The least squares adjustment vector and its corresponding variance-covariance matrix for station position and orbital estimated for each independent daily solution were then passed to a Kalman filter GLOBK (Herring *et al.*, 1990) to perform a global network adjustment, and to estimate station positions and their formal errors. I imposed the reference frame by minimizing position and velocity deviations of IGS stations with respect to the ITRF2000, while estimating orientation, translation, and scale transformation.

#### 4. Time series and velocities field

Processing the above GPS data yielded the precise coordinates of all stations. Here, the horizontal and vertical velocities were calculated by linear fitting. Fig. 5 shows some examples of the time series. In this figure each small solid circle on the plot represents an independent position estimate, typi-



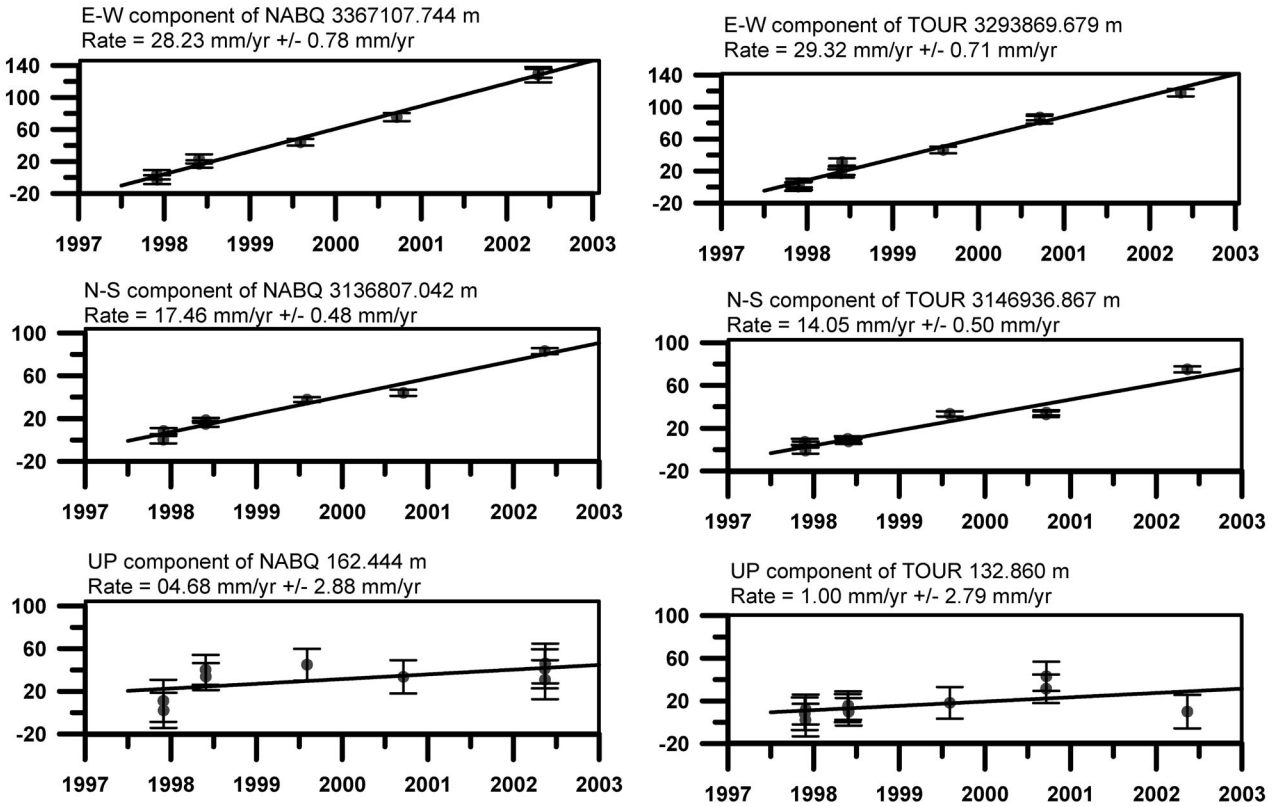


Fig. 5 a~c. Some examples of time series of station positions (mm) with respect to ITRF2000. Small solid circles on the plot represent an independent position estimate, typically based on 24 hours of observations, with error bars indicating  $\pm$  one standard error.

cally based on 24 hours of observations, with error bars indicating  $\pm$  one standard error. Even though repeatability in the vertical component is much poorer, some significant tectonic displacements were found (Fig. 5). The seven IGS stations mentioned were selected to establish a common reference frame for the observational GPS campaigns. These stations have RMS in each velocity component that is smaller than 1.0 mm/yr in the ITRF2000 reference frame. Calculated horizontal velocity field in ITRF2000 is found to be in the range of 29.0~35.0 mm/yr with an average of 31.2 mm/yr at  $N60^{\circ}E$ . The associated standard deviation of the velocities ranges from 0.5 to 1.2 mm/yr for horizontal components and from 2.4 to 5.8 mm/yr for vertical components (Table 1). Then, I used the estimated Euler vectors of the Eurasian plate relative to ITRF2000 of Prawirodirdjo and Bock (2004) (longitude  $-99.691^{\circ}E$ , latitude  $57.246^{\circ}N$ ,  $\omega$  0.26 deg/Myr) to convert the velocity vectors into a kinematic reference frame. Fig. 6 shows the observed horizontal velocity vectors with error ellipses relative

to the Eurasian plate. Because most of the coordinate time series are well approximated by the linear fitting method used in this study, we may consider that the horizontal velocities shown in Fig. 6 are representative of the present secular deformation of the Gulf of Suez-Sinai region. The horizontal components of these velocity vectors are further used to estimate the strain field by the Least-Squares Prediction method.

## 5. Strains analysis

Monitoring crustal strain perturbations is the key to understanding physical processes in the crust, as well as to forecast crustal activity. Dense GPS measurements with a long time span provide us with one of the ideal tools to realize this. In the present study, I try to delineate the crustal strain of the Gulf of Suez-Sinai Peninsula using GPS measurements for the period from 1997 to 2002, and discuss its tectonic implications.

To delineate crustal strains in the Gulf of Suez-

Table 1. Station coordinates, observed ITRF2000 velocities, and  $1\sigma$  uncertainties.  
\*IGS sites used in this study.

Site	Longitude, °E	Latitude, °N	Velocity		
			East	North	Vertical
DAHA	34.47	28.529	26.49 ± 1.38	20.06 ± 1.07	6.99 ± 5.87
NABQ	34.314	28.178	28.49 ± 1.1	19.56 ± 0.61	4.68 ± 2.88
SHAM	34.184	27.846	33.42 ± 1.25	16.51 ± 0.92	4.63 ± 4.91
CATH	33.995	28.639	29.89 ± 1.13	18.37 ± 0.78	-1.98 ± 3.7
KENS	33.883	27.961	26.17 ± 1.11	20.05 ± 0.72	-2.18 ± 3.22
HURG	33.832	27.244	26.55 ± 1.15	17.12 ± 0.68	0.73 ± 2.85
TOUR	33.596	28.269	29.68 ± 1.07	15.97 ± 0.64	1.00 ± 2.79
GEMS	33.494	27.686	27.31 ± 1.06	17.84 ± 0.60	4.07 ± 2.48
DERB	33.404	28.631	27.12 ± 1.09	16.87 ± 0.64	4.49 ± 2.75
ZIET	33.391	27.919	27.79 ± 1.14	18.59 ± 0.75	-0.65 ± 3.48
GARB	33.228	28.163	27.28 ± 1.07	19.5 ± 0.58	1.59 ± 2.48
BAHR*	50.608	26.209	31.33 ± 0.39	26.35 ± 0.32	-1.6 ± 0.94
ANKR*	32.758	39.887	12.61 ± 0.40	-2.91 ± 0.26	-0.05 ± 0.98
MADR*	355.75	40.429	20.04 ± 0.46	14.16 ± 0.26	0.15 ± 1.18
MAS1*	344.367	27.764	18.47 ± 0.41	18.89 ± 0.38	1.8 ± 1.1
MALI*	40.194	-2.996	25.12 ± 0.86	13.36 ± 0.54	1.5 ± 1.15
RAMO*	34.763	30.598	19.43 ± 0.80	14.23 ± 0.41	1.9 ± 1.42
HARK*	27.708	-25.887	16.49 ± 0.76	19.79 ± 0.67	-1.9 ± 1.43

Sinai region, I applied the Least-Squares Prediction (LSP) method. The LSP method is a part of the least-squares collocation (LSC) method developed by Moritz (1962) for reducing gravity data, and has been applied to crustal deformation data by El-Fiky *et al.* (1997). In the LSC, the data vector  $l$  is assumed to be composed of systematic errors, tectonic signal, and noise, and can be expressed by the following observation equation ;

$$l = AX + t + n.$$

Where  $A$  is a design matrix,  $X$  represents model parameters for network adjustment,  $t$  is the signal vector, and  $n$  is the noise vector. In the present study, I use the above estimated horizontal velocity vectors as the primary data set (Fig. 6). I use the LSP method to interpolate the velocities to a uniform 4 km × 4 km grid, from which I can then compute the principle components of strain.

In the above equation, noise comprises erroneous fluctuations that are inherent at each of the GPS sites. A number of error sources can affect the GPS coordinate estimates, which then propagate into the velocity estimates, including : global errors (orbits and terrestrial references frame, e.g., Blewitt, 1993), regional errors, especially tropospheric refraction (e.g., Davis *et al.*, 1985), and local, site-specific errors

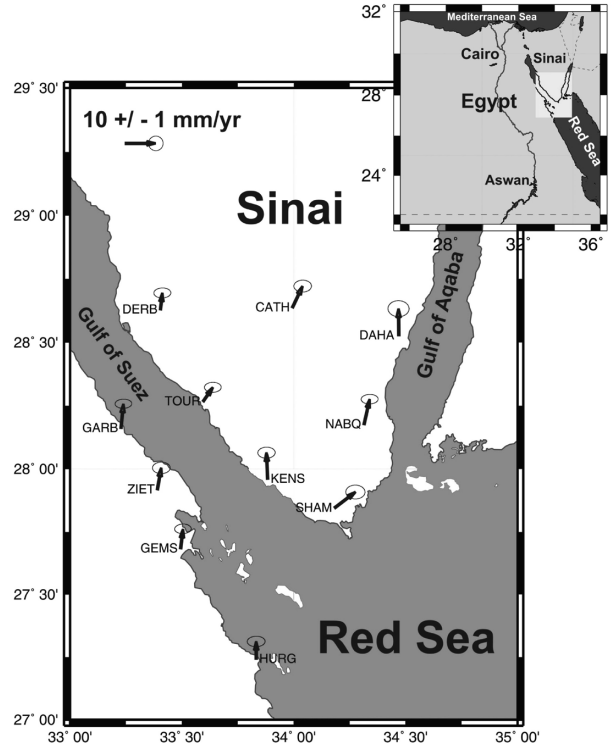


Fig. 6. Yearly averaged velocity vectors with error ellipses obtained from repeated GPS measurements relative to the ITRF2000 reference frame in the Suez-Sinai region for the period 1997~2002.

including monument instability, multipath, and signal scattering. (e.g., Genrich and Bock, 1992). Such errors or noise have to be removed to obtain tectonic crustal deformation. Some researchers have used spatial filtering of common-mode noise in geodetic time series to reduce global errors (e.g., Wdowinski *et al.*, 1997). In this study I use El-Fiky and Kato (1999)'s approach. I perform a variance-covariance analysis to determine empirically the spatial correlation inherent in the velocity field. I assume that there are no systematic errors in the present velocity estimates ( $AX=0$ ), so I am only left with a tectonic signal,  $t$ , and random noise,  $n$ . Here, noise is assumed to comprise local errors that are limited only to the GPS site or its adjacent local area, while the tectonic signal can have wider spatial correlations. I further assume that the velocity field is isotropic and homogeneous, so the covariances of data are only functions of site distance (e.g., El-Fiky *et al.*, 1997 ; El-Fiky and Kato, 1999). I then demean the EW and NS velocity components, and calculate variance  $C_i(0)=(\sum l_i l_i)/N$  and covariance  $C_i(d_q)=(\sum l_i l_j)/N_q$  of the data for each component. Here,  $N$  is the total number of data sites and  $N_q$  is the number of data points within a specific discrete distance interval, from which  $d_q$  is taken as the median of this assumed interval. Variances are estimated at each observational site, whereas covariances are estimated for all site pairs within the assigned distance interval. Thus, variances  $C_i(0)$  obtained may include signal and noise, but covariances  $C_i(d_q)$  include only signals according to the above hypothesis.

A plot of the covariances with respect to distance would be a curve that naturally diminishes with distance. One simple mathematical function to express such plots would be a Gaussian function in the following form,  $C_i(d_i)=C_i(0) \exp(-k^2 d_i^2)$ , which I chose here as the empirical covariance function (ECF). Two parameters  $C_i(0)$  and  $k$  are fitted from a covariance plot of the data.  $C_i(0)$  is the expected variance at the sites and  $C_i(0)-C_i(0)$  is considered to be the noise component at the site.  $k$  is an indication of how far the correlation reaches, which has the dimension of the inverse distance.

Once ECF is obtained, we can estimate the signal  $S$  at any arbitrary point using the following formula (e.g., El-Fiky and Kato, 1999) ;

$$S=C_{st}C_L^{-1}L.$$

Where the matrix  $C_{st}$  is composed of elements  $c_{st}$  ( $1 \leq t \leq N, 1 \leq s \leq P$ , where  $P$  is the number of grid points whose signals are to be estimated) ;  $c_{st}$  is given by  $c_{st}=C_{ut}(0) \exp(-k_u^2 d_{st}^2)$  for EW component and  $c_{st}=C_{vt}(0) \exp(-k_v^2 d_{st}^2)$  for NS component, respectively, where  $d_{st}$  is distance between data site and predicted site. The above formula was used to reconstruct velocity vectors (signal) at grid points ( $4 \text{ km} \times 4 \text{ km}$ ) throughout the study region.

## 6. Results and discussion

To estimate the crustal strains in the GPS data for the period (1997~2002), I used the horizontal velocity vectors shown in Fig. 6. The averages of velocities in the NS and EW components are subtracted separately from all of the site velocities to remove systematic bias. Then, I applied the LSP as described above to each vector component (East-West and North-South) independently. ECF for each component are fitted to the data. The parameters of  $k_{ub}$ ,  $C_{ub}$ , and  $C_{ur}$  for the EW component are estimated to be  $0.0209 \text{ km}^{-1}$ ,  $16.85 \text{ (mm/yr)}^2$ , and  $10.11 \text{ (mm/yr)}^2$ , respectively. While the  $k_{vb}$ ,  $C_{vb}$ , and  $C_{vr}$  parameters for the NS component are estimated to be  $0.0198 \text{ km}^{-1}$ ,  $7.35 \text{ (mm/yr)}^2$ , and  $10.1 \text{ (mm/yr)}^2$ , respectively. These parameters are used to compose the covariances matrices, and reconstruct displacement vectors (signal) at grid points in the Gulf of Suez-Sinai peninsula region. Then, the estimated velocities at these grid points are differentiated in space to obtain crustal strains in this data period.

Figures 7, 8, and 9 are the estimated areal dilational strains, maximum shear strains, and principal axes of strains, respectively. The results obtained in these figures might portray tectonic strains in the Gulf of Suez-Sinai region.

First, the dilatational strains shown in Fig. 7 indicate that the region under study is separated into two areas : the eastern part where compression strain is predominant and the western part along the Gulf of Suez where extensive areal strain prevails. The largest areal compressions reach more than  $0.3 \text{ ppm/yr}$  in the northern part of the Gulf of Aqaba, which might be attributed to compressional activity along the plate boundary between the Arabian and African plates, the Dead Sea fault. The extensional strain

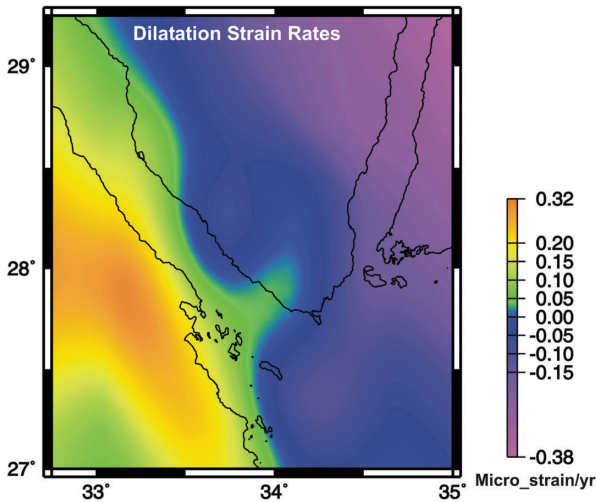


Fig. 7. The areal dilatation of the Suez-Sinai area as estimated by the LSP technique for the period 1997~2002. Unit is Micro-strain/yr.

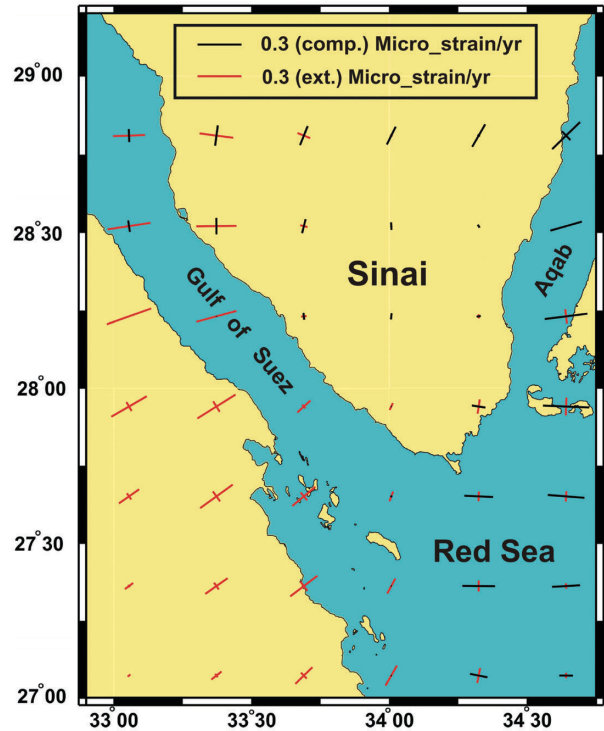


Fig. 9. Magnitude and orientation of rates of principal strains axes on the Suez-Sinai area as estimated by LSP for the period 1997~2002.

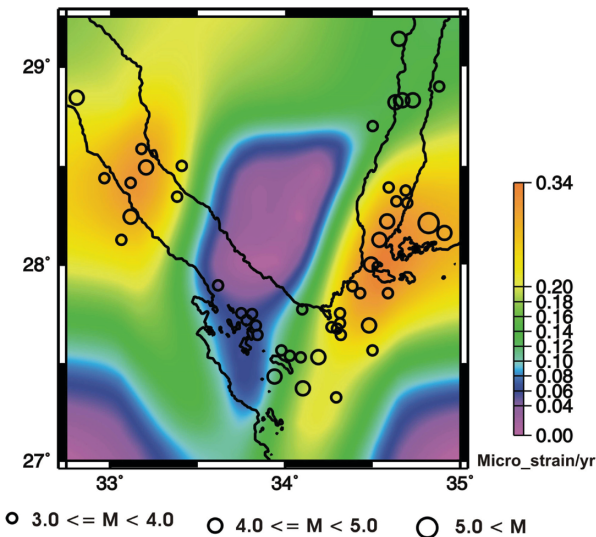


Fig. 8. Distribution of maximum shear strain rates in the Suez-Sinai area as estimated by LSP for the period 1997~2002. Unit is Micro-strain/yr. Epicenters of shallow earthquakes ( $d < 30$  km) determined by NEIC are also plotted.

along the Gulf of Suez and its western coast might have contributed to the opening of the Gulf of Suez as indicated by several tectonic studies (e.g., Steckler *et al.*, 1988 ; Le Pichon and Gaulier, 1988).

Maximum shear strain is mostly accommodated at the Gulf of Suez to the west, and where the Gulf of Aqaba begins in the eastern part of the region under study. In addition, there is a low maximum shear strain zone in the middle of the region under study

between the Gulf of Suez and the Gulf of Aqaba. The estimated maximum shear strain rate in the area under study is about 0.25 Micro-strain/yr on average. The strain field in the two maxima areas might not relate to any co-seismic and/or post-seismic movements. The seismicity of the study area was low during the period of interest ; the largest magnitude of earthquake recorded was less than 5.3 near the Gulf of Aqaba (Fig. 8). To compare the maximum shear strains with the seismic data, the epicenters of shallow earthquakes with depths less than 30 km are plotted in the Fig. 8. As can be seen in this figure, the distribution of seismicity shows high consistency with high shear strain areas. The low strain rates and low level of earthquake occurrence at the central part of the area under study (Figs. 3 and 8) indicate that internal deformation in this region is very small. This is in good agreement with the results obtained by Wdowski *et al.*, (2004). They used continuous GPS observations around the middle of the Dead Sea Fault for the period from 1996 to 2001 to monitor current crustal deformation across the Dead Sea Fault. Their analysis indicates that the stations located west of the Dead Sea Fault show no significant

motion with respect to the Sinai sub-plate, suggesting the rigid behavior of Sinai plate. Whereas the stations located east of the Dead Sea Fault show a significant slow motion with respect to the Sinai block, indicating a left-lateral motion along the Dead Sea Fault.

The present analysis shows that the African coast side and the Gulf of Suez are dominated by extensional strain rates. The extensional axes of strains change direction gradually from E-W in the northern part of the Gulf of Suez to a more northerly direction toward the NE-SW to the south along the southern part of the Suez Gulf and the coast of the African side (Fig. 9). The estimated extensional strain rate is about 0.30 Micro-strain/yr on average. The extensional strain in this region might be due to the extensional force acting along the Gulf of Suez and the northern part of Red Sea. In contrast, in the eastern part of the study area (along the Gulf of Aqaba and in northern part of the Red Sea), compressional strain is evident (Fig. 9). The compressional axes of strains tend to rotate gradually from E-W in the northern part of the Red Sea and the southern part of the Gulf of Aqaba to a more northerly direction toward the NE-SW to the north along the gulf. This might be due to compressional force acting at the plate boundary between the Arabian and African plates. The principal axes of strains show a good correlation with the  $S_{Hmax}$  directions obtained from earthquake focal mechanisms and borehole breakouts. Badawy (2001) used earthquake focal mechanisms and borehole breakouts in Egypt, and compiled a stress field for Egypt including the region under study. His results show dominant NW-SE compression in and around the Gulf of Suez. Along the southern and central parts of the Dead Sea Fault the direction is changing from NW-SE to NNW-SSE. Mahmoud (2003) also estimated the spatial distribution of the stress axes from the focal mechanisms of moderate to large earthquakes. His results are similar to those of Badawy (2001). In spite of the scatter of seismic data and the uneven distribution of sampling sites, the direction of contraction is in general agreement with the strain rate field derived from GPS (Fig. 9).

The recent seismicity of the Sinai Peninsula proves that most of its activity is inter-plate rather than intra-plate (Fig. 3), so we can define Sinai as a sepa-

rate sub-plate, as it shows more rigid behavior. The sub-plate can deform in its interior only if the force distribution varies laterally along boundaries, but this deformation might occur as a result of aseismic or seismic movements. Previous studies in this area (e.g., Riguzzi *et al.*, 1999 ; Piersanti *et al.*, 2001) attribute the internal low gradient deformation inside Sinai to aseismic movements, which reflects the low seismicity inside Sinai micro-plate. This agrees with the strains patterns obtained in the present study. Ben-Menahem *et al.* (1976) and Salamon *et al.* (1996) considered the Sinai Peninsula to be a sub-plate (splinter) of the African plate, which is breaking up incoherently as it approaches the collision zone with the Eurasian plate.

To define Sinai boundaries, earthquake activity and tectonic setting of the Aqaba-Levant Fault trend prove that this major trend represents the eastern margin of Sinai sub-plate. Some authors (e.g. McKenzie, 1970, 1972 ; Kempler and Ben-Avraham, 1987 ; Kempler and Garfunkel, 1991), consider the Cyprian Arc zone of convergence to be a boundary separating the Sinai sub-plate from the Anatolian plate. The western boundary of the Sinai sub-plate is not defined well as there is no tectonic (Garfunkel and Bartov, 1977), morphologic, or seismic (Salamon *et al.*, 1996) evidence for the northward continuation of the Suez Rift toward the Cyprian Arc. Mascle *et al.* (2000) defined an active fault belt that might correspond to an offshore extension of the Suez Rift, and suggested that this belt represents the western boundary of the Sinai sub-plate. Recently, Bosworth and McClay (2001) suggested it was a continuation of the Suez Rift northward, via a regional left-stepping relay beneath the Nile Delta. The focal mechanisms of the 1999 December 28 sequence, northeast of Cairo (Badawy and Abdel Fattah, 2001), of March 1984 (Salamon *et al.*, 2003) support this suggestion of Bosworth and McClay (2001).

Badawy and Horvath (1999) suggested a kinematic model of the Sinai sub-plate region on the basis of earthquake distribution, satellite images, geological information, and previous discussions. According to this model the Sinai region is considered to be a sub-plate that is partially separated from the African plate by the Suez rift. The earthquake activity in the Gulf of Suez and Gulf of Aqaba regions is a direct consequence of the relative motions of African plate,

Sinai, and Arabia. The Sinai sub-plate got its present configuration from the Late Miocene when motion jumped from the Suez rift to the Aqaba-Dead Sea transform fault system. The model proposed by Badawy and Horvath (1999) suggests that the Dead Sea Fault adapts to the relative motion between the Sinai and Arabia, and continues to the north. The earthquake distribution shows that the southern segment of the Dead Sea Fault runs NW to the Mediterranean (Roum fault) south of Beirut (Lebanon). During this phase of motion (10 Ma) the total displacement is about 72 km with a slip rate of 7.2 mm/yr. The displacement along the active branch of the Dead Sea strike-slip fault was resolved by the Syrian arc system. Their model actually offers an alternate view of the formation of the northern segment of the Dead Sea Fault system. The northward propagation of the Dead Sea Fault system in Lebanon and Syria, (northern segment) started only from Pliocene. This phase occurred during the last 5 Ma since Pliocene by the same rate of 7.2 mm/yr. Therefore, the total displacement along it should be only 35 km. This assumption solves one of the major difficulties relating to the Dead Sea Fault system, which is the difference in the total displacement along the southern and northern segments. Their model predicts a normal extensional motion in the Gulf of Suez with a minor left-lateral strike-slip component. The present study clearly shows the opening of the Gulf of Suez. This is consistent with Badawy and Horvath (1999)'s model.

Although I believe that it is not possible to draw an exhaustive geodynamical conclusion from these limited GPS surveys, I emphasize that our results are consistent with the extensional motion at the Gulf of Suez, as inferred from geological and seismological investigations. On the other hand, the lack of GPS data on the Arabian Peninsula makes the discussion along the Gulf of Aqaba incomplete.

More repeated analyses with longer time intervals are required to clarify whether or not detectable deformation in the area is due to seismic or even aseismic deformation. On the other hand, to add to our knowledge of the kinematics of this region it would be useful to have data from additional GPS sites located on the Arabian Peninsula. Finally, as mentioned earlier, monitoring variations of crustal strains in space and time in such an active tectonic

region is the key to understanding the physical process in the crust, and to forecasting crustal activity. A dense array of continuous GPS tracking networks supplemented by a dense seismic network could provide us with an ideal tool to achieve this. For this purpose the National Research Institute of Astronomy and Geophysics (NRIAG), Egypt, has installed a modern seismic network, and is planning to establish dense arrays of continuous GPS tracking networks in Egypt.

## 7. Conclusion

GAMIT and GLOBK software packages have been used to analyze GPS measurements in the western coast of Gulf of Suez and the southern part of Sinai Peninsula, Egypt. Velocity vectors obtained in ITRF2000 indicate that the magnitude of the horizontal velocity is in the range of 29–35 mm/yr with an average of 31.2 mm/yr at N60°E. The associated errors are about 2.0 mm and 1.0 mm in the east and north components, respectively. I first applied the least-squares prediction method to segregate signal and noise from velocity vectors. Estimated horizontal signals (horizontal displacement rates) were then differentiated in space to calculate the principal components of strains. Dilatations, maximum shear strains, and principal axes of strains clearly portray the tectonic environments of the Sinai area. (1) Dilatational strains indicate that the area under study can be divided into two regions: the eastern region along the Aqaba Gulf where compression strain is predominant and the western region along the Gulf of Suez where extensive areal strain prevails. (2) Maximum shear strains show a good agreement with the distribution of seismicity in the area. (3) Principal axes of the strains indicate that the Gulf of Suez is under the influence of extensional forces acting in the NE-SW direction. Moreover, the principal axes of strains correlate with the directions of compressional axes of stresses obtained from earthquake focal mechanisms and borehole breakouts.

## Acknowledgments

The author is very grateful to the staff of National Research Institute of Astronomy and Geophysics, Helwan, Cairo, Egypt, who participated in the GPS data campaigns used in this study. The author is also very grateful to Prof. Teruyuki Kato

for his help and useful discussions during the author's stay at the Earthquake Research Institute. Comments by Dr. Yosuke Aoki and Dr. Takeshi Iinuma were invaluable to improve the manuscript. A GMT software package was used to plot some figures in this paper.

## References

- Altamimi, Z., P. Sillard and C. Boucher (2002), ITRF2000 : A new release of the International Terrestrial Reference Frame for Earth science application, *J. Geophys. Res.*, 107, 2214, doi : 10, 1029/2001JB000561.
- Ambraseys, N.N., Melville, C.P. and Adam, R.D., 1994. The Seismicity of Egypt, Arabia and the Red Sea : a historical review. Cambridge University Press, Cambridge.
- Badawy, A. (2001), The present-day stress field in Egypt. *Annali di Geofisica*, 44, 3, 557–570.
- Badawy, A. and A.K. Abdel Fattah, (2001), Source parameters and fault plane determinations of the 28 December 1999 northeastern Cairo earthquakes, *Tectonophysics*, 343, 6377.
- Badawy, A. and F. Horvath, (1999), The Sinai subplate and tectonic evolution of the northern Red Sea region, *Geodynamics*, 27, 433,, 450.
- Ben-Avraham, Z., (1978), The structure and tectonic setting of the Levant continental margin, eastern Mediterranean, *Tectonophysics*, 46, 313±331.
- Ben-Menahem, A., Nur, A. and M. Vered, (1976), Tectonics, seismicity, and structure of the afro-Eurasian junction—the breaking of an incoherent plate, *Phys. Earth planet. Inter.*, 12, 1±50.
- Blewitt, G., (1993), Advances in Global Positioning System technology for geodynamics investigations : 1978–1992, In *Contributions of Space Geodesy to Geodynamics Technology* edited by D.E. Smith and D.L. Turcotte, pp. 195–213.
- Bosworth, W. and K. McClay, (2001), Structural and stratigraphic evolution of the Gulf of Suez rift, Egypt : a synthesis, in *Peri-Tethys Memoir 6, Peri-Tethyan rift/wrench basins and passive margins*. *Memoires du Museum National d'Histoire Naturelle de Paris*, Vol. 186, pp. 567606, eds Ziegler, P.A., Cavazza, W., Robertson, A. H.F. and Crasquin-Soleau, S.
- Courtilot, V., R. Armijo and P. Tapponier, (1987), The Sinia triple junction revisited, *Tectonophysics*, 141, 181–190.
- Davis, J.L., T.A., Herring, I.I. Shapiro, A.E.E., Rogers and G., Elgered, (1985), Geodesy by radio interferometry : effects of atmospheric modeling errors on estimates baselines length, *Radio Sci.*, 20, 1593–1607.
- DeMets, C., Gordon, R.G., Argus, D.F., S. and Stein, (1990), Current plate motions, *Geophys. J. Int.*, 101 : 425–478.
- DeMets, C., R.G. Gordon, D.F. Argus and S. Stein, (1994), Effects of recent revisions to the geomagnetic reversal time scale on estimates of current plate motions, *Geophys. Res. Lett.*, 21, 2191–2194.
- Dixon, T.H. and M.P. Golombek, (1988), Late Precambrian crustal accretion rates in northeast Africa and Arabia. *Geology*, 16, 991–994.
- El-Fiky, G.S., (2000), Crustal strains in the Eastern Mediterranean and Middle East as derived from GPS Observations, *Bull. Earthquake Research Institute, Univ. of Tokyo, Japan*, V. 75, No. 2, 161–181.
- El-Fiky, G.S. and T. Kato, (1999), Continuous distribution of the horizontal strain in the Tohoku district, Japan, deduced from least squares prediction. *J. Geodynamics*, 27 : 213–236.
- El-Fiky, G.S., T. Kato and Y. Fujii, (1997), Distribution of the vertical crustal movement rates in the Tohoku district, Japan, predicted by least-squares collocation, *J. of Geodesy*, 71 : 432–442.
- Garfunkel, Z., (1981), Internal structure of the Dead Sea leaky transform (rift) in relation to plate kinematics, *Tectonophysics*, 80, 81–108.
- Garfunkel, Z. and Y. Bartov, (1977), The tectonics of the Suez rift. *Geol. Surv. Israel. Bull.*, 71, 44.
- Genrich, J.F. and Y. Bock, (1992), Rapid resolution of crustal motion at short ranges with Global Positioning System, *J. Geophys. Res.*, 97, 3261–3269.
- Herring, T.A., J.L. Davis and I.I. Shapiro, (1990). Geodesy by radio interferometry : The application of Kalman filtering to the analysis of very long baseline interferometry data. *J. Geophys. Res.*, 95, 12561–12581.
- Jestin, F., P. Hunchon and J.M. Gaulier, (1994), The Somalia plate and the East African rift system : Present-day kinematics, *Geophys. J. Int.*, 116, 637–654.
- Kato, T., G.S. El-Fiky, E.N. Oware and S. Miyazaki, (1998), Crustal strain in the Japanese islands as deduced from GPS dense array, *Geophys. Res. Lett.*, 25 : 3445–3448.
- Kebeasy R., (1990), Seismicity. In *The Geology of Egypt* Edited by Said R., 51–59, Balkema, Rotterdam.
- Kempler, D. and Z. Ben-Avraham, (1987), The tectonic evolution of the Cyprean arc, *Ann. Tectonicae* 1, 58–71.
- Kempler, D. and Z., Garfunkel, (1991), The northeast Mediterranean triple junction from a plate kinematic point of view, *Bull. Tech. Univ., Istanbul*, 44, 203–232.
- Kimata, F., A. Tealeb, H. Murakami, N. Furukawa, S. Mahmoud, H. Khalil, K. O. Sakr and A. M. Hamdy, (1997), The Aqaba earthquake of 22 November 1995 and co-seismic deformation in Sinai Peninsula deduced from repeated GPS measurements. *Acta Geod. Geophys. Hung.* 32 (1–2), 53–71.
- King, R.W. and Y. Bock, (1997), Documentation for the MIT GPS analysis software. *Mass. Inst. of Technol., Cambridge*.
- Le Pichon, X. and J.M. Gaulier, (1988), The rotation of Arabia and the Levant fault system, *Tectonophysics* 153, 271–294.
- Mahmoud, S., (2003), Seismicity and GPS-derived crustal deformation in Egypt, *Geodynamics*, 35, 333–352.
- Masce, J., J. Benkheilil, G. Bellaiche, T. Zitter, J. Woodside and L. Loncke, (2000), Marine geologic evidence for a Levantine-Sinai Plate, a new piece of the Mediterranean puzzle, *Geology*, 28, 779–782.
- McClusky, S., S. Balassanian, A. Barka, C. Demir, S. Ergintav, I. Georgiev, O. Gurkan, M. Hamburger, K. Hurst, H. Kahle, K. Kastens, G. Kekelidze, R. King, V. Kotzev, O. Lenk, S. Mahmoud, A. Mishin, M. Nadariya, A. Ouzounis, D. Paradissis, Y., Peter, M. Prilepin, R., Reilinger, I. Sanli, H. Seeger, A. Tealeb, M.N. Toksoz and G. Veis,

- (2000), Global Positioning System constraints on plate kinematics and dynamics in the Eastern Mediterranean and Caucasus, *J. Geophys. Res.*, 105, 5695–5719.
- McKenzie, D.P., (1970), Plate tectonics of the Mediterranean region, *Nature*, 226, 239–243.
- McKenzie, D.P., (1972), Active tectonics of the Mediterranean region, *Geophys. J. R. Astron. Soc.*, 30, 109–185.
- Moritz, H., (1962), Interpolation and prediction of gravity and their accuracy, Report No. 24, Inst. Geod. Phot. Cart., The Ohio State Univ., Columbus, U.S.A.
- Piersanti, A., C. Nostro and F. Riguzzi, (2001), Active displacement field in Suez-Sinai area : the role of postseismic deformation, *Earth and Planet. Science Lett.*, 193, 13–23.
- Prawirodirdjo, L. and Y. Bock, (2004), Instantaneous global plate motion model from 12 years of continuous GPS observations, *J. Geophys. Res.*, 109, B08405.
- Riguzzi, F., S.M. Mahmoud and A. Tealeb, (1999), Displacement pattern of the Sinai area : first results from GPS. *Annali Di Geofisica* 42 (4).
- Salamon, A., A. Hofstetter, Z. Garfunkel and H. Ron, (1996), Seismicity of the eastern Mediterranean region, Perspective from the Sinai subplate, *Tectonophysics*, 263, 293–305.
- Salamon, A., A. Hofstetter, Z. Garfunkel and H. Ron, (2003), Seismotectonics of Sinai subplate —eastern Mediterranean region, *Geophys. J. Int.*, 155, 149–173.
- Steckler, M.S., (1985), Uplift and extension at the Gulf of Suez : indications of induced mantle convection, *Nature* 317, 135–139.
- Steckler, M.S., F. Berthelot, N. Liberis and X. Le Pichon, (1988), Subsidence in the Gulf of Suez : implications for rifting and plate kinematics, *Tectonophysics* 153, 249–270.
- Wdowinski, S., Y. Bock, G. Baer, L. Prawirodirdjo, N. Bechor, S. Naaman, R. Knafo, Y. Forrai and Y. Melzer, (2004), GPS measurements of current crustal movements along the Dead Sea Fault, *J. Geophys. Res.*, 109, B05403.
- Wdowinski, S., Y. Bock, J. Zhang, R. Knafo and J. Genrich, (1997), Southern California permanent GPS geodetic arrays : spatial fettering of daily position for estimating coseismic and postseismic displacements induced by the 1992 Lander earthquake, *J. Geophys. Res.*, 102, 18,057–18,070.

(Received October 1, 2005)

(Accepted March 10, 2006)